

Enigmatic Solar Wind Disappearance Events – Do We Understand Them?

Janardhan P.

Physical Research Laboratory, Ahmedabad 380 009, India.

e-mail: jerry@prl.res.in

Abstract. At the Sun–Earth distance of one astronomical unit (1 AU), the solar wind is known to be strongly supersonic and super Alfvénic with Mach and Alfvén numbers being on average 12 and 9 respectively. Also, solar wind densities (average $\sim 10 \text{ cm}^{-3}$) and velocities (average $\sim 450 \text{ km s}^{-1}$) at 1 AU, are known to be inversely correlated with low velocities having higher than average densities and *vice versa*. However, on May 11 and 12 1999 the Earth was engulfed by an unusually low density ($< 0.1 \text{ cm}^{-3}$) and low velocity ($< 350 \text{ km s}^{-1}$) solar wind with an Alfvén Mach number significantly less than 1. This was a unique low-velocity, low-density, sub-Alfvénic solar wind flow which spacecraft observations have shown lasted more than 24 hours. One consequence of this extremely tenuous solar wind was a spectacular expansion of the Earth’s magnetosphere and bow shock. The expanding bow shock was observed by several spacecraft and reached record upstream distances of nearly 60 Earth radii, the lunar orbit. The event was so dramatic that it has come to be known as *the solar wind disappearance event*. Though extensive studies of this event were made by many authors in the past, it has only been recently shown that the unusual solar wind flows characterizing this event originated from a small coronal hole in the vicinity of a large active region on the Sun. These recent results have put to rest speculation that such events are associated with global phenomenon like the periodic solar polar field reversal that occurs at the maximum of each solar cycle. In this paper we revisit the 11 May 1999 event, look at other disappearance events that have occurred in the past, examine the reasons why speculations about the association of such events with global phenomena like solar polar field reversals were made and also examine the role of transient coronal holes as a possible solar source for such events.

Key words. Solar wind disappearance—polar field reversals—transient coronal holes—active regions.

1. Introduction

The origin of low-speed solar wind flows has recently been of great interest because, unlike its high speed counterpart that emanates only from large open field regions

called coronal holes, the low-speed solar wind can have different origins. Low speed solar wind is known to be associated with small mid-latitude coronal holes and it has been shown that solar wind speeds are inversely correlated with the expansion factors of magnetic flux tubes, with lower speeds coming from regions having large magnetic flux expansion factors and *vice versa* (Wang & Sheeley 1990; Sheeley *et al.* 1991). Low-speed solar wind outflows are also known to emanate from the tops of closed coronal loops in helmet streamers, from the outer boundaries of closed loop regions in active regions (Wang *et al.* 1998), and from small coronal holes in the vicinity of large active regions (Kojima *et al.* 1999). A high correlation has also been found (Nolte *et al.* 1976; Neugebauer *et al.* 1998) between solar wind speed and the size of the coronal hole from which it originates.

The extremely spectacular nature of the so-called solar wind disappearance event of 11 May 1999 has caused it to be one of the most extensively studied and reported solar wind related events in recent times. A number of observations have been reported using both space-based and ground-based instrumentation (Crooker *et al.* 2000; Farrugia *et al.* 2000; Richardson *et al.* 2000; Usmanov *et al.* 2000; Vats *et al.* 2001; Balasubramanian *et al.* 2003). Until very recently however, none of these authors were able to explain the cause or locate the solar source of the event. Many authors had speculated (Usmanov *et al.* 2000; Balasubramanian *et al.* 2003; Usmanov *et al.* 2003) that the event was somehow related to large scale solar phenomena like the periodic solar polar field reversal and had raised questions about how the solar wind could be turned off for a period of 24 hours or more. Recently, Janardhan *et al.* (2006), have been able to locate a solar source of this unusual event and have put to rest speculation about the event being associated with large scale solar phenomena like the periodic solar polar field reversal that takes place at the maximum of each solar cycle.

2. Solar wind disappearance events

As stated earlier, disappearance events are characterised by extremely low velocities and low densities. A few such events have been reported earlier, with the earliest reported case being that of the long duration density depletion in the interplanetary medium (Schwenn 1983; Gosling *et al.* 1982) which was observed by Helios 1 and Helios 2 spacecraft. The event occurred in November 1979, during solar maximum in cycle 21 and was as dramatic as the May 1999 event with proton densities decreasing steadily over an entire day from the normal value of $\sim 100 \text{ cm}^{-3}$ to less than 1 cm^{-3} , at about 0.3 AU the Helios 1 perihelion. The velocity and the magnetic field, during the same period, remained constant at 300 km s^{-1} and 35 nT, respectively. Schwenn (1983) has noted that there was no disturbance in the interplanetary medium for several days ahead of the density drop nor was there any associable solar surface feature. Usmanov *et al.* (2003) have scanned through the OMNI and ACE spacecraft databases from 1962 to 2002 and have selected those events that have densities of 0.4 cm^{-3} or less and have found a total of 18 such events. Of these 18 events, 7 including the 11 May 1999 event during Carrington Rotation 1949 (CR1949), were found to have minimum density values of 0.2 cm^{-3} or less. Table 1 shows these seven events from Usmanov *et al.* (2003). The last column in table 1 is the Alfvén Mach number and it can be seen that all the 7 events are sub-Alfvénic.

Table 1. Disappearance events with densities $\leq 0.2 \text{ cm}^{-3}$.

Date (yyyy:mm:dd)	Rotation	Day number	ρ_{\min} (cm^{-3})	Alfvén Mach No. ($M_{A \min}$)
1977:10:18	1660	293	0.2	0.79
1979:07:04	1683	185	0.1	0.61
1979:07:31	1684	212	0.2	0.68
1979:11:22	1688	326	0.1	0.54
1999:05:11	1949	131	0.02	0.41
2002:03:20	1987	79	0.14	0.50
2002:05:24	1990	144	0.07	0.54

3. Spacecraft and ground based observations of the May 1999 event

The first panel (top) of Fig. 1 shows a synoptic map for CR1949 in May 1999 made using magnetograms from the MDI instrument onboard SOHO. Heliographic longitude is marked at the top while CMP dates are marked at the bottom of the map. Regions of large magnetic field strength, corresponding to active region locations are shown as black and white patches to distinguish the two magnetic polarities. The curved solid line is the magnetic neutral line. Converging black lines on the map join magnetic fields on the source surface at $2.5R_{\odot}$, derived from potential field computations (Hakamada & Kojima 1999), with their corresponding counterparts on the photosphere. The potential field lines that are marked in white correspond to fields with CMP date of 11 May 1999 and lie within the two solid, vertically oriented, parallel lines that bracket the traceback location of day-of-year 131 (DOY 131) corresponding to 11 May 1999. Also shown by thick white lines are the locations of CH boundaries inferred from HeI 10830 Å observations. The second panel shows a map of the magnetic flux expansion rates with the white, light-grey, dark-grey and black regions corresponding to flux expansion rates of > 1000 , between 100 and 1000, between 10 and 100 and between 1 and 10 respectively. The third panel shows a tomographic synoptic velocity map projected on the source surface at $2.5R_{\odot}$ for CR1949 in May 1999, obtained using Interplanetary Scintillation (IPS) data from the four-station solar wind observatory of the Solar Terrestrial Environment Laboratory (STEL), Toyokawa, Japan. The dashed white and black lines, in panel three, demarcate respectively, the boundaries of the low velocity flows ($< 400 \text{ km s}^{-1}$) and polar coronal hole boundaries. Dates of CMP are indicated at the bottom of the map with the corresponding heliographic longitudes marked at the top of the map. The path of the ACE spacecraft is indicated by a thick line along the equator. The lower panel shows ACE *in situ* measurements of proton velocities that have been mapped back along Archimedean spirals to the source surface at $2.5R_{\odot}$. The two sets of solid and dashed vertical parallel lines running across all the panels demarcate respectively, the back projected location of DOY 131 when the solar wind flow was highly non-radial and days on either side of DOY 131 when the solar wind flow was radial. The dashed vertical parallel lines therefore represent the maximum possible errors in the back projected solar source locations. Details of how the flux expansion rates are computed and a complete description of the errors in the back projection of ACE velocities from 1 AU to the source surface at $2.5R_{\odot}$ can be seen in Janardhan *et al.* (2006). It is clear from Fig. 1 (uppermost panel) that

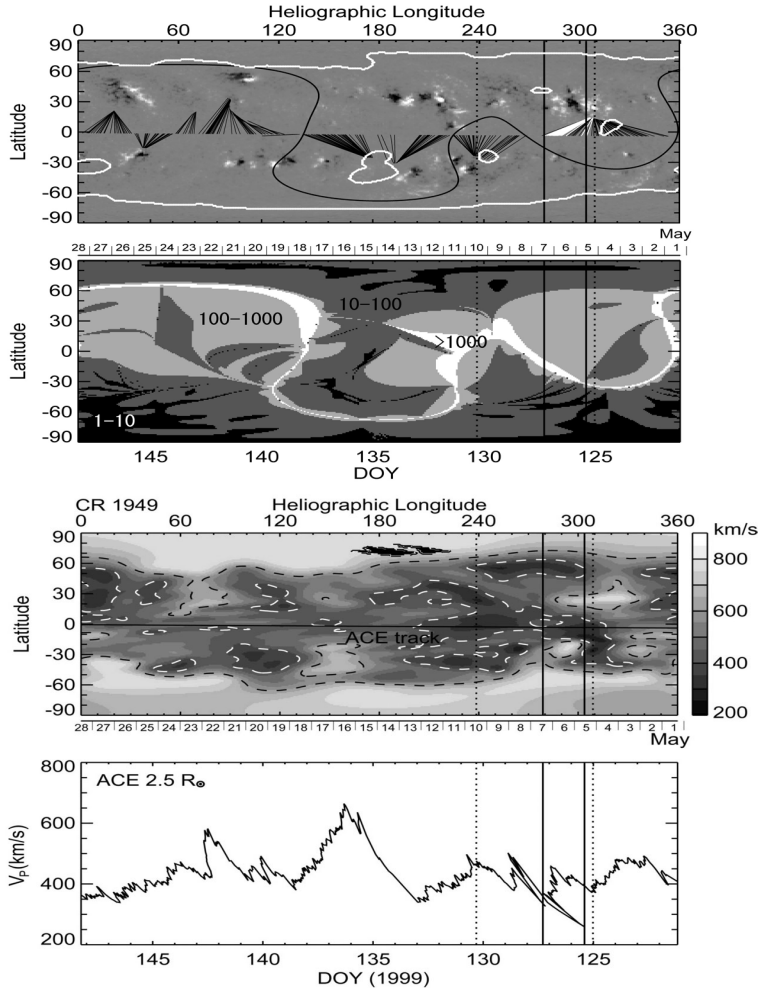


Figure 1. The uppermost panel shows a synoptic map for CR1949 in May 1999 made using magnetograms from the MDI instrument onboard SOHO. Heliographic longitude is marked at the top while CMP dates are marked at the bottom of the map. Regions of large magnetic field strength, corresponding to active region locations, are shown as black and white patches to distinguish the two magnetic polarities. The curved solid line is the magnetic neutral line. Converging black lines on the map join magnetic fields on the source surface at $2.5R_{\odot}$, derived from potential field computations with their corresponding counterparts on the photosphere. The potential field lines that are marked in white correspond to fields with CMP date of 11 May 1999. Shown by thick white lines are the locations of CH boundaries. The second panel shows a map of the magnetic flux expansion rates with the white, light-grey, dark-grey and black regions corresponding to flux expansion rates of > 1000 , between 100 and 1000, between 10 and 100 and between 1 and 10 respectively. The third panel shows a tomographic synoptic IPS velocity map projected on the source surface at $2.5R_{\odot}$ for CR1949 in May 1999. The dashed white and black lines, in panel three, demarcate respectively, the boundaries of the low velocity flows and polar coronal hole boundaries. The path of the ACE spacecraft is indicated by a thick line along the equator. The lowermost panel shows ACE in situ measurements of proton velocities that have been mapped back along Archimedean spirals to the source surface at $2.5R_{\odot}$. The two sets of solid and dashed vertical parallel lines running across all the panels demarcate respectively, the back projected location of DOY 131 when the solar wind flow was highly non-radial and days on either side of DOY 131 when the solar wind flow was radial.

the solar wind observed at 1 AU during the solar wind disappearance event originated from the vicinity of the large active region complex (AR8525) located at around 18° N, and between Heliographic longitudes 280° and 300° . Janardhan *et al.* (2006) have shown that the interplanetary magnetic field during the event was stable and unipolar, thereby implying a coronal hole origin for the solar wind flows, and have argued that the low density, low velocity flows originated from the small mid latitude coronal hole located close to the potential field lines marked in white in Fig. 1. Janardhan *et al.* (2006) have also argued that the small size of the coronal hole and the large magnetic flux expansion factors from the region could adequately explain the low velocities produced. They have further proposed an interesting method for producing the low densities, by assuming that rearrangements in CH boundaries would produce a pinch-off or separation of the solar wind outflow, thereby completely detaching the outflow from its solar source. They have argued that if such a detached outflow occurred within ~ 48 hours of its start and it continued to expand as it propagated out to 1 AU, an increase in its radius by a factor of 6–7 would lead to a decrease in densities by a factor of ~ 200 –300 at 1 AU. Thereby, typical particle densities of approximately 20 – 30 particles cm^{-3} at 0.5 AU could be reduced to 0.1 particles cm^{-3} at 1 AU given that the typical travel time between the sun and the earth, at these low velocities, is ~ 5 days. It is important to bear in mind here that the large active region complex (AR8525) would have been located at central meridian approximately 5 days before 11 May 1999 thereby producing earth directed outflows.

4. Discussion and conclusions

4.1 Transient coronal hole

Apart from small mid-latitude coronal holes, another class of coronal holes are the so-called transient coronal holes (TCH) which were first discovered in Skylab data (Rust 1983). These TCH are short lived (≤ 2 days) regions of dimmed X-ray intensity which are sometimes observed in association with CMEs. However, coronal radiation responsible for HeI 10830 \AA comes from higher altitudes than soft X-ray emission and thus represent larger spatial scales. HeI 10830 \AA observations of coronal hole boundaries will therefore be blurred and cannot be used to detect the smallest CHs or TCH which are generally small in size. Even at soft X-ray wavelengths, since the corona is optically thin, foreground and background emission can prevent the detection of TCH on the limb thereby limiting TCH detections to those that are well away from the limb. Thus, detecting TCH would require special and careful processing of soft X-ray and EUV data.

In an extensive study of 19 TCH, using 9 years of data from the YOHKOH soft X-ray telescope (SXT), Kahler & Hudson (2001) have shown that TCH:

- are small in size,
- have short lifetimes;
- occur in magnetic unipolar regions trailing large active regions,
- generally occur at regions where the magnetic neutral line shows large scale curvature.

Also, the typical lifetimes of TCHs of ~ 48 hours as compared to typical travel times between the sun and 1 AU of 3–5 days for the solar wind, implies that outflows

originating at a small TCH can become totally disconnected from the source. The stable and uni-polar nature of the flows from the vicinity of AR8525 and the central meridian location of AR8525 taken together with the extensive and detailed work by Kahler & Hudson (2001) described above indicate that transient coronal holes could be an alternative solar source for explaining other such low velocity, tenuous solar wind flows seen at 1 AU. From Fig. 1 (upper panel) we can see that the solar wind flows of 11 May 1999 originated from a small area on the sun trailing AR8525 and the magnetic neutral line showed a large curvature. It is therefore not unreasonable to speculate that the other tenuous solar wind outflows listed in Table 1 could have probably originated in small TCH. The small area of the TCH associated with such an outflow would produce very low velocities (Wang & Sheeley 1990; Sheeley *et al.* 1991; Nolte *et al.* 1976; Neugebauer *et al.* 1998). The typical lifetime of a TCH of ~ 2 days as compared to solar wind travel time of ~ 5 days would imply that the low velocity flow from the TCH would have been completely detached from the solar surface approximately three days before reaching 1 AU and after propagating roughly 40% of the distance to earth orbit. As described earlier a simple expansion of this large detached low velocity flow region, as it propagated out to 1 AU, could give rise to an extremely low density cloud that engulfs the earth.

Four of the events listed in Table 1 have occurred close to the solar maximum while the remaining have occurred well within two years of the maximum when solar activity was still high. The fact that disappearance events seemed to occur at or around solar maximum when solar polar field reversals are taking place led to speculation that the large-scale restructuring of the solar magnetic fields during solar polar field reversals, is likely to be associated with density anomalies in the solar wind. The current work indicates that the connection of such events with polar field reversal periods is incidental in that the solar maximum period is dominated by large active regions and a highly deformed neutral line configuration, thereby maximizing the likelihood for the formation of small TCH (Kahler & Hudson 2001) and/or small mid latitude CH. Also, mid latitude and equatorial coronal holes are nearly absent during the solar minimum phase thereby increasing the likelihood of such events being observed only at or around solar maximum. Finally, spacecraft observations are confined to the ecliptic, another reason for observing such events at or around solar maximum because of the increased probability for the occurrence of mid-latitude and equatorial coronal holes during solar maximum.

Since coronal hole boundaries locate separatrices of coronal magnetic fields which in turn define its large-scale current systems, this work has also highlighted the need for systematic studies of the dynamics and evolution of CH boundaries. Such studies could help define coronal hole boundary structure and help in understanding boundary field connectivities. Regular and systematic observations by both ground and space based platforms will be required to identify many more such events and ground-based IPS observations will be of value in such future studies.

5. Acknowledgements

The author thanks the ACE SWEPAM instrument team and the ACE Science Center for making ACE Level 2 data available in the public domain via the World Wide Web. The author acknowledges support provided by a three-month visiting position during 2003, at the Solar-Terrestrial Environment Laboratory, Toyokawa, Japan during

which this work was carried out. The author also thanks Fujiki, K., Kojima, M., and Tokumaru, M., from the Solar Terrestrial Environment Laboratory, Toyokawa, Japan for discussions and help in this work.

References

- Balasubramanian, V., Janardhan, P., Srinivasan, S., Ananthakrishnan, S. 2003, IPS observations of the solar wind disappearance event of May 1999; *J. Geophys. Res.*, **108**, 1121–1131.
- Crooker, N. U., Shodhan, S., Gosling, J. T., Simmerer, J., Lepping, R. P., Steinberg, J. T., Kahler, S. W. 2000, Density extremes in the solar wind; *Geophys. Res. Lett.*, **27**, 3769–3772.
- Farrugia, C. J., Singer, H. J., Evans, D., Berdichevsky, D., Scudder, J. D., Ogilvie, K. W., Fitzenreiter, R. J., Russell, C. T. 2000, Response of the equatorial and polar magnetosphere to the very tenuous solar wind on May 11, 1999; *Geophys. Res. Lett.*, **27**, 3773–3776.
- Gosling, J.T., Asbridge, J. R., Bame, S. J., Feldman, W. C., Zwickl, R. G., Pashmann, G., Sckopke, N., Russell, C. T. 1982, A sub-Alfvénic solar wind: interplanetary and magnetosheath observations; *J. Geophys. Res.*, **87**, 239–245.
- Hakamada, K., Kojima, M. 1999, Solar wind speed and expansion rate of the coronal magnetic field during carrington rotation 1909; *Solar. Phys.*, **187**, 115–122.
- Janardhan, P., Fujiki, K., Kojima, M., Tokumaru, M., Hakamada, K. 2006, Resolving the enigmatic solar wind disappearance event of May 1999; *J. Geophys. Res.*, **110**, A08101.
- Kahler, S. W., Hudson, H. S. 2001, Origin and development of transient coronal holes; *J. Geophys. Res.*, **106**, 29,239–29,248.
- Kojima, M., Fujiki, K., Ohmi, M., Tokumaru, M., Yokobe, A., Hakamada, K. 1999, Low speed solar wind from the vicinity of solar active regions; *J. Geophys. Res.*, **104**, 16,993–17,003.
- Neugebauer, M., Forsyth, R. J., Galvin, A. B., Harvey, K. L., Hoeksema, J. T., Lazarus, A. J., Lepping, R. P., Linker, J. A., Mikic, Z., Steinberg, J. T., von Steiger, R., Wang, Y.-M., Wimmer-Schweingruber, R. F. 1998, Spatial structure of the solar wind and comparisons with solar data and models; *J. Geophys. Res.*, **103**, 14,587–14,600.
- Nolte, J. T., Krieger, A. S., Timothy, A. F., Gold, R. E., Roelof, E. C., Vaiana, G., Lazarus, A. J., Sullivan, J. D., McIntosh, P. S. 1976, Coronal holes as sources of solar wind; *Sol. Phys.*, **46**, 303–322.
- Richardson, I. G., Berdichevsky, D., Desch, M. D., Farrugia, G. J. 2000, Solar-cycle variation of low density solar wind during more than 3 solar cycles; *Geophys. Res. Lett.*, **27**, 3761–3764.
- Rust, D. M. 1983, Coronal Disturbances and their Terrestrial Effects; *Space Sci. Rev.*, **34**, 21–24.
- Schwenn, R. 1983, The average solar wind in the inner heliosphere: structure and slow variations; *Solar Wind 5 [NASA Conf. Pub. 2280]*, (ed.) M. Neugebauer, pp. 489–508.
- Sheeley, N. R. Jr., Swanson, E. T., Wang, Y.-M. 1991, Out of the ecliptic tests of the inverse correlation between solar wind speed and coronal expansion factor; *J. Geophys. Res.*, **96**, 13,861–13,868.
- Usmanov, A. V., Goldstien, M. L., Farrell, W. M. 2000, A view of the inner heliosphere during the May 10–11, 1999 low density anomaly; *Geophys. Res. Lett.*, **27**, 3765–3768.
- Usmanov, A. V., Farrell, W. M., Ogilvie, K. W., Goldstien, M. L. 2003, The sub-Alfvénic solar wind and low density anomalies; *Proc. EGS-AGU-EUG Joint Assembly*.
- Vats, H. O., Sawant, H. S., Oza, R., Iyer, K. N., Jadhav, R. 2001, Interplanetary scintillation observations of the solar wind disappearance event of May 1999; *J. Geophys. Res.*, **106**, 25,121–25,124.
- Wang, Y.-M., Sheeley Jr. 1990, Solar wind speed and coronal flux-tube expansion; *Astrophys. J.*, **355**, 726–732.
- Wang, Y.-M., Sheeley, N. R. Jr., Walters, J. H., Brukner, G. E., Howard, R. A., Michels, D. J., Lamy, P. L., Schwenn, R., Simnett, G. M. 1998, Origin of streamer material in the outer corona; *Astrophys. J.*, **498**, L165–L168.